Effects of saturation in the transient process of a dye laser. II. Colored-noise case

Li Cao and Da-jin Wu*
Chinese Center of Advanced Science and Technology (World Laboratory), P.O. Box 8730 Beijing, 100 080, People's Republic of China and Department of Physics and National Laboratory of Laser Technology, Huazhong University of Science and Technology, Wuhan 430 074, People's Republic of China†

Xue-li Luo
Department of Physics, Huazhong University of Science and Technology, Wuhan 430 074, People's Republic of China
(Received 6 November 1991)

We have derived the approximate formulas of the mean, variance, and skewness of the first-passage-time distribution for the colored-loss-noise model and the colored-gain-noise model of the dye laser by virtue of the best Fokker-Planck-equation approximation. Comparing the colored-loss-noise model with the colored cubic model, it is shown that our analytic results are in good agreement with the numerical simulation given by Zhu, Yu, and Roy [Phys. Rev. A **34**, 4333 (1986)]. We find that the prefactor of the pump fluctuation term can curb the variance and skewness of the first-passage-time distribution. In the regime $0.8 < I_0 < 1$, where I_0 denotes the relative laser intensity, the best Fokker-Planck equation predicts that as the laser intensity is increased, the increases of the variance and skewness of the first-passage-time distribution for the colored saturation models are slower than those of corresponding white saturation models.

PACS number(s): 42.55.Mv, 42.50.Md, 42.50.Lc

I. INTRODUCTION

In the previous paper [1] (referred to as paper I), we have discussed the effects of saturation in the single-mode dye laser driven by white noise. In the present study, effects of saturation in the transient process for the single-mode dye laser driven by colored noise are discussed. In this paper, we have used the best Fokker-Planck equation (BFPE) [2] to treat this problem. The reasons for this are as follows. First, in view of this we will discuss two dye-laser models which contain saturation terms; the BFPE approximation can treat these models without encountering the difficulty of negative diffusion functions. Second, the BFPE method can be used in the case in which the correlation time of the colored noise is larger than or equal to the laser gain relaxation time. Third, the diffusion functions given by this method turn out to be phase independent. Therefore, the evolution of the laser intensity can be decoupled from the phase.

The purpose of paper I is to calculate the mean, variance, and skewness of first-passage-time distribution (FPTD) for the single-mode dye-laser models with saturation terms driven by white noise. In that paper, a comparison with the cubic model driven by the white noise is made. Since the pump noise for the dye laser is, in reality, colored, the purpose of the present paper is to calculate the corresponding quantities for single-mode dye-laser models with saturation terms driven by colored noise, and then make a comparison between these models containing the cubic model driven by colored noise.

The paper is arranged as follows. In Sec. II, we present the two-dimensional Langevin equations for models A and B. In Sec. III, the BFPE associated with these Langevin equations is given. Section IV is devoted to the discussion of the diffusion functions. In Sec. V, we calculate the above-mentioned quantities for the models. Finally, the conclusions are presented in Sec. VI.

II. LANGEVIN EQUATIONS

A. Loss-noise model (model A)

The equation of motion of this model for the complex field amplitude $E=E_1+iE_2$ of a single-mode dye laser is given by the stochastic differential equation (SDE) [3]

$$\frac{\partial E}{\partial t}=-KE+\Gamma\frac{E}{1+k|E|^2}+p(t)E+q(t)\ , \tag{1}$$

where K is the cavity decay rate, $\Gamma=a_0+K$ is the gain factor, a_0 is the net gain, $k\equiv A/\Gamma$, and A is the laser self-saturation coefficients. The effects of spontaneous emission on the laser field E are represented by the quantum noise $q(t)=q_1+iq_2$ which are assumed to be the Gaussian white noise with zero mean and the correlation function

$$\langle q_i(t)q_j(t')\rangle=p\delta_{ij}\delta(t-t')\quad(i,j=1,2) \tag{2}$$

in which P is the strength of the quantum noise. The turbulence in the dye jet and pump laser noise may be represented by the pump fluctuations $p(t)=p_1+ip_2$, which are Ornstein-Uhlenbeck noises with zero mean and the correlation function

$$\langle p_i(t)p_j(t')\rangle=\delta_{ij}\left[\frac{p'}{2\tau}\right]e^{-|t-t'|/\tau}\quad(i,j=1,2)\ . \tag{3}$$

Here P' is the strength of the pump fluctuations and τ is the correlation time of the fluctuations. δ_{ij} is the

Kronecker symbol and K, Γ, A, τ, P, and P' are real parameters.

The change of variables to polar coordinates according to

$$E=xe^{i\phi}=\sqrt{I}e^{i\phi} \tag{4}$$

allows us to rewrite (1) as

$$\frac{dx}{dt}=-(\Gamma-a_0)x+\Gamma\frac{x}{1+x'^2}+p_1(t)x +q_1(t)\cos\phi+q_2(t)\sin\phi\ , \tag{5}$$

$$\frac{d\phi}{dt}=p_2(t)-\frac{1}{x}q_1(t)\sin\phi+\frac{1}{x}q_2(t)\cos\phi\ , \tag{6}$$

where $x'^2=kx^2=kI$ and I denotes the intensity. Notice that (5) and (6) are the full two-dimensional Langevin equations for the dye laser. One can rewrite (5) and (6) in the matrix form as

$$\frac{d}{dt}\begin{bmatrix}x\\ \phi\end{bmatrix}=\begin{bmatrix}-(\Gamma-a_0)x+\Gamma\dfrac{x}{1+x'^2}\\ 0\end{bmatrix}+\begin{bmatrix}x & 0\\ 0 & 1\end{bmatrix}\begin{bmatrix}p_1\\ p_2\end{bmatrix} +\begin{bmatrix}\cos\phi & \sin\phi\\ -\dfrac{1}{x}\sin\phi & \dfrac{1}{x}\cos\phi\end{bmatrix}\begin{bmatrix}q_1\\ q_2\end{bmatrix}\ . \tag{7}$$

By introducing the vectors

$$y=\begin{bmatrix}x\\ \phi\end{bmatrix}\ ,\mathbf{p}(t)=\begin{bmatrix}p_1(t)\\ p_2(t)\end{bmatrix}\ ,\mathbf{q}(t)=\begin{bmatrix}q_1(t)\\ q_2(t)\end{bmatrix}$$

and

$$\mathbf{G}(\mathbf{y})=\begin{bmatrix}-(\Gamma-a_0)x+\Gamma\dfrac{x}{1+x'^2}\\ 0\end{bmatrix} \tag{8}$$

and the matrices

$$\underline{g}^c(\mathbf{y})=\begin{bmatrix}x & 0\\ 0 & 1\end{bmatrix}\ , \tag{9}$$

$$\underline{g}^w(\mathbf{y})=\begin{bmatrix}\cos\phi & \sin\phi\\ -\dfrac{1}{x}\sin\phi & \dfrac{1}{x}\cos\phi\end{bmatrix}\ , \tag{10}$$

one can rewrite (7) as

$$\dot{\mathbf{y}}=\mathbf{G}(\mathbf{y})+\underline{g}^c(\mathbf{y})\mathbf{p}(t)+\underline{g}^w(y)\mathbf{q}(t)\ . \tag{11}$$

This is the two-dimensional Langevin equation for model A. The superscripts c and w denote, respectively, the functional coefficients of the colored and white fluctuations.

B. Gain-noise model (model B)

The corresponding SDE for model B is [2]

$$\frac{\partial E}{\partial t}=-(\Gamma-a_0)E+\Gamma\frac{E}{1+k|E|^2}+\frac{E}{1+k|E|^2}p(t)+q(t)\ . \tag{12}$$

Similarly, (12) can be rewritten in the following form:

$$\frac{dx}{dt}=-(\Gamma-a_0)x+\Gamma\frac{x}{1+kx^2}+\frac{x}{1+kx^2}p_1(t) +q_1(t)\cos\phi+q_2(t)\sin\phi\ , \tag{13a}$$

$$\frac{d\phi}{dt}=\frac{1}{1+kx^2}p_2(t)-\frac{1}{x}q_1(t)\sin\phi+\frac{1}{x}q_2(t)\cos\phi\ . \tag{13b}$$

The matrix form of (13) is

$$\frac{d}{dt}\begin{bmatrix}x\\ \phi\end{bmatrix}=\begin{bmatrix}-(\Gamma-a_0)x+\Gamma\dfrac{x}{1+kx^2}\\ 0\end{bmatrix}+\begin{bmatrix}\dfrac{x}{1+kx^2} & 0\\ 0 & \dfrac{1}{1+kx^2}\end{bmatrix}\begin{bmatrix}p_1(t)\\ p_2(t)\end{bmatrix}+\begin{bmatrix}\cos\phi & \sin\phi\\ -\dfrac{1}{x}\sin\phi & \dfrac{1}{x}\cos\phi\end{bmatrix}\begin{bmatrix}q_i(t)\\ q_2(t)\end{bmatrix}\ . \tag{14}$$

Similarly, it can also be written in the form of (11) by introducing the vectors

$$\mathbf{y}=\begin{bmatrix}x\\ \phi\end{bmatrix}\ ,\quad \mathbf{p}(t)=\begin{bmatrix}p_1(t)\\ p_2(t)\end{bmatrix}\ ,\quad \mathbf{q}(t)=\begin{bmatrix}q_1(t)\\ q_2(t)\end{bmatrix}\ ,$$

and

$$\mathbf{G}(\mathbf{y})=\begin{bmatrix}-(\Gamma-a_0)x+\Gamma\dfrac{x}{1+x'^2}\\ 0\end{bmatrix} \tag{15}$$

and the matrices

$$\underline{g}^c(\mathbf{y})=\frac{1}{1+x'^2}\begin{bmatrix}x & 0\\ 0 & 1\end{bmatrix}\ , \tag{16}$$

$$\underline{g}^w(\mathbf{y})=\begin{bmatrix}\cos\phi & \sin\phi\\ -\dfrac{1}{x}\sin\phi & \dfrac{1}{x}\cos\phi\end{bmatrix}\ . \tag{17}$$

III. BEST FOKKER-PLANCK EQUATION

In this section we derive the BFPE associated with the two-dimensional Langevin equations (7) and (14) [2]. The Liouville operator L_0 associated with the systematic portion of the Langevin equations and the corresponding operators L_c and L_w associated with the stochastic portions of the equations are [2]

$$L_0=-\nabla_{\mathbf{y}}\cdot\mathbf{G}(\mathbf{y})\ , \tag{18}$$

$$L_c(t)=-\nabla_y\cdot\underline{g}^c(\mathbf{y})\mathbf{p}(t)\ , \tag{19}$$

$$L_w(t)=-\nabla_y\cdot\underline{g}^w(\mathbf{y})\mathbf{q}(t)\ , \tag{20}$$

where $\nabla_y\equiv(\partial/\partial x,\partial/\partial\phi)$. The corresponding BFPE can be derived from [2]

$$\frac{\partial}{\partial t}W_t=-\nabla_y\cdot\mathbf{G}(\mathbf{y})W_t+\frac{P}{2}[\nabla_y\cdot\underline{g}^w(\mathbf{y})]^T[\nabla_y\cdot\underline{g}^w(\mathbf{y})]W_t+\int_0^t dt'\langle L_c(t)e^{L_0t'}L_c(t-t')e^{-L_0t'}\rangle\times W_t[1+O(p'\tau)]\ , \tag{21}$$

where $W_t\equiv W(\mathbf{y},t|\mathbf{y}_0)$ is the conditional probability density and T denotes the transpose. In the following we derive the BFPE for models A and B.

A. Model A

The first, second, and third terms on the right-hand side of (21) for model A are

$$-\nabla_y\cdot\mathbf{G}(\mathbf{y})W_t=-\frac{\partial}{\partial x}\left[-(\Gamma-a_0)x+\Gamma\frac{x}{1+x'2}\right]W_t\ , \tag{22}$$

$$[\nabla_y\cdot\underline{g}^w(\mathbf{y})]^T[\nabla_y\cdot\underline{g}^w(\mathbf{y})]W_t=\left[\frac{\partial^2}{\partial x^2}-\frac{\partial}{\partial x}\frac{1}{x}+\frac{1}{x^2}\frac{\partial^2}{\partial\varphi^2}\right]W_t\ , \tag{23}$$

and

$$\int_0^t dt'\langle L_0(t)e^{L_0t'}L_c(t-t')e^{-L_0t'}\rangle W_t=\sum_{i,j,K,S}\frac{\partial}{\partial y_i}g^c_{ij}(\mathbf{y})\frac{\partial}{\partial y_K}g^c_{KS}(\mathbf{y})D_{Sj}(\mathbf{y},t)W_t \tag{24}$$

with $(i,j,K,S=1,2)$, where $D_{ij}(\mathbf{y},t)$ are the diffusion functions $D_{12}=D_{21}=0$, $D_{11}=D_{11}(x)$, and $D_{22}=D_{22}(x)$. These show that the diffusion functions are independent of the phase ϕ. We will discuss the diffusion functions in detail in Sec. IV.

Substituting (9) into (24), we obtain

$$\int_0^t dt'\langle L_c(t)e^{L_0t'}L_c(t-t')e^{-L_0t'}\rangle W_t=\frac{\partial}{\partial x}x\frac{\partial}{\partial x}xD_{11}(x)W_t+\frac{\partial^2}{\partial\phi^2}D_{22}(x)W_t=\frac{\partial}{\partial x}x\frac{\partial}{\partial x}xD_{11}(x)W_t+D_{22}(x)\frac{\partial^2}{\partial\phi^2}W_t\ . \tag{25}$$

Using Eqs. (22), (23), and (25), the BFPE associated with the two-dimensional Langevin equation (7) is obtained from (21):

$$\frac{\partial}{\partial t}W_t=-\frac{\partial}{\partial x}\left[-(\Gamma-a_0)x+\Gamma\frac{x}{1+x'^2}\right]W_t+\frac{P}{2}\frac{\partial^2}{\partial x^2}W_t-\frac{P}{2}\frac{\partial}{\partial x}W_t+\frac{P}{2}\frac{1}{x^2}\frac{\partial^2}{\partial\phi^2}W_t+\frac{\partial}{\partial x}x\frac{\partial}{\partial x}xD_{11}(x)W_t+D_{22}(x)\frac{\partial^2}{\partial\phi^2}W_t\ . \tag{26}$$

It is noteworthy that due to the phase independence of the diffusion functions $D_{ii}(x)$ one can eliminate the angle variable ϕ by integrating Eq. (26). We thus define a reduced probability density

$$Q_t\equiv Q(x,t|x_0)\equiv\frac{1}{2\pi}\int_0^{2\pi}d\phi\int_0^{2\pi}d\phi_0W(x,\phi,t|x_0,\phi_0)\ . \tag{27}$$

Now, by virtue of (27), we get from (26) an evolution equation for Q_t:

$$\frac{\partial Q_t}{\partial t}=-\frac{\partial}{\partial x}\left[-(\Gamma-a_0)x+\Gamma\frac{x}{1+x'^2}\right]Q_t+\frac{P}{2}\frac{\partial^2}{\partial x^2}Q_t-\frac{P}{2}\frac{\partial}{\partial x}\frac{1}{x}Q_t+\frac{\partial}{\partial x}x\frac{\partial}{\partial x}xD_{11}(x)Q_t\ . \tag{28}$$

B. Model B

for model B, the explicit formulas of the first, second, and third terms on the right-hand side of (21) are obtained from (14):

$$\nabla_y\cdot\underline{G}(\mathbf{y})W_t=\frac{\partial}{\partial x}\left[-(\Gamma-a_0)x+\Gamma\frac{x}{1+x'^2}\right]W_t\ , \tag{29}$$

$$[\nabla_y\cdot\underline{g}^w(\mathbf{y})]^T[\nabla_y\cdot\underline{g}^w(\mathbf{y})]W_t=\left[\frac{\partial^2}{\partial x^2}-\frac{\partial}{\partial x}\frac{1}{x}+\frac{1}{x^2}\frac{\partial^2}{\partial\varphi^2}\right]W_t\ , \tag{30}$$

and

$$\int_0^t dt'\langle L_c(t)e^{L_0t'}L_c(t-t')e^{-L_0t'}\rangle W_t=\frac{\partial}{\partial x}\frac{x}{1+x'^2}\frac{\partial}{\partial x}\frac{x}{1+x'^2}D_{11}(x)W_t+D_{22}(x)\frac{\partial^2}{\partial\varphi^2}W_t\ . \tag{31}$$

We note that for model B the diffusion functions are the same as for model A.

From (29)–(31) and (21), we obtain the BFPE associated with the two-dimensional Langevin equation (14):

$$\frac{\partial W_t}{\partial t}=-\frac{\partial}{\partial x}\left[(a_0-\Gamma)x+\Gamma\frac{x}{1+x'^2}\right]W_t+\frac{P}{2}\frac{\partial^2}{\partial x^2}W_t-\frac{P}{2}\frac{\partial}{\partial x}\frac{1}{x}W_t+\frac{\partial}{\partial x}\frac{x}{1+x'^2}\frac{\partial}{\partial x}\frac{1}{1+x'^2}D_{11}(x)W_t+\frac{P}{2}\frac{1}{x^2}\frac{\partial^2}{\partial\varphi^2}W_t+D_{22}(x)\frac{1}{1+x'^2}\frac{\partial^2}{\partial\phi^2}W_t\ . \tag{32}$$

The reduced probability density Q_t for model B obeys the evolution equation

$$\frac{\partial Q_t}{\partial t}=-\frac{\partial}{\partial x}\left[(a_0-\Gamma)x+\Gamma\frac{x}{1+x'^2}\right]Q_t+\frac{P}{2}\frac{\partial^2}{\partial x^2}Q_t-\frac{P}{2}\frac{\partial}{\partial x}\frac{1}{x}Q_t+\frac{\partial}{\partial x}\frac{x}{1+x'^2}\frac{\partial}{\partial x}\frac{x}{1+x'^2}D_{11}(x)Q_t\ . \tag{33}$$

IV. DIFFUSION FUNCTIONS

In this section, we calculate the diffusion functions $D_{ij}(x,t)$ and discuss the effect of the ratio $\Gamma/(\Gamma-a_0)$ on the $D_{ij}(x,t)$. According to the theory of the BFPE, the diffusion functions are given by [2]

$$D_{ij}(x,t)=\int_0^t dt' H_{ij}(x,t')\frac{P'}{2\tau}e^{-t'/\tau}, \tag{34}$$

where the functions $H_{ij}(\mathbf{y},t)$ satisfy the partial differential equation [2]

$$\frac{\partial H_{ij}}{\partial t}=\sum_{K,l,S}\left[(g^c)^{-1}_{il}\left[\frac{\partial G_l}{\partial x_K}\right]g^c_{KS}H_{Sj}-(g^c)^{-1}_{il}\left[\frac{\partial g^c_{lS}}{\partial x_K}\right]H_{Sj}G_K\right]-\sum_K\left[\frac{\partial H_{ij}}{\partial x_K}\right]G_K \tag{35}$$

with the initial condition

$$H_{ij}(\mathbf{y},0)=\delta_{ij}. \tag{36}$$

It is shown that model A and model B have the same H_{ij} since both models have the same $G(\mathbf{y})$. The differential of $g^c(\mathbf{y})$ of models A and B does not influence the functions H_{ij}.

The solutions of this partial differential equation are

$$H_{ij}(\mathbf{y},t)=0 \quad \text{for } i\neq j \tag{37}$$

and

$$H_{22}(\mathbf{y},t)=1 \tag{38}$$

and $H_{11}(\mathbf{y},t)$ can only be written in general in terms of a transcendental equation:

$$a_0H_{11}^{\Gamma/(\Gamma-a_0)}-[a_0-(\Gamma-a_0)x'^2]H_{11}^{[\Gamma/(\Gamma-a_0)]-1}=(\Gamma-a_0)x'^2e^{-2a_0t}. \tag{39}$$

An explicit solution is only possible for particular values of the parameters.

If $\Gamma/(\Gamma-a_0)\gg 1$, we have from (39)

$$H_{11}=e^{-2(\Gamma-a_0)t}, \tag{40}$$

and if $\Gamma/(\Gamma-a_0)=1$, we find

$$H_{11}=1. \tag{41}$$

In the cases $\Gamma/(\Gamma-a_0)=1.5$ and 2, in order to obtain explicit solutions of (39), it is necessary to make some approximations. Therefore, we use the value at the stationary state $x'_{SS}=a_0/(\Gamma-a_0)$ to replace x'^2 in (39). The function H_{11} is then given by

$$H_{11}=e^{-(\Gamma-a_0)^{2/3}t} \quad \text{when} \quad \frac{\Gamma}{\Gamma-a_0}=1.5 \tag{42a}$$

and

$$H_{11}=e^{-(\Gamma-a_0)t} \quad \text{when} \quad \frac{\Gamma}{\Gamma-a_0}=2. \tag{42b}$$

The diffusion functions associated with these H_{ij} can be obtained by virtue of (34). When the correlation time τ is short, it is usually argued that the upper limit in the integration in (34) can be set to infinity, and the diffusion functions thus become independent of time [4–7]. The off-diagonal diffusion functions vanish because of (37). The result (38) immediately yields $D_{22}(x)=P'/2$. Using (40)–(42) and (34), the function $D_{11}(x)$ is given by

$$D_{11}=P'/2 \quad \text{when} \quad \frac{\Gamma}{\Gamma-a_0}=1, \tag{43}$$

$$D_{11}=\frac{P'/2}{1+\frac{2}{3}(\Gamma-a_0)\tau} \quad \text{when} \frac{\Gamma}{\Gamma-a_0}=1.5, \tag{44}$$

$$D_{11}=\frac{P'/2}{1+(\Gamma-a_0)\tau} \quad \text{when} \frac{\Gamma}{\Gamma-a_0}=2, \tag{45}$$

$$D_{11}=\frac{P'/2}{1+2(\Gamma-a_0)\tau} \quad \text{when} \frac{\Gamma}{\Gamma-a_0}>3. \tag{46}$$

Equations (43), (44), and (45) approximately correspond to the three different pump levels (a) $a_0=2.16\times10^6$ sec^{-1}, (b) $a_0=4.32\times10^6$ sec^{-1}, and (c) $a_0=8.64\times10^6$ sec^{-1} in set B of the experimental data (see Ref. [8]).

V. MEAN, VARIANCE, AND SKEWNESS OF FPTD

A. Model A

If D_{11} is denoted as $P'_e/2$, the BFPE (28) can be rewritten as

$$\frac{\partial Q_t}{\partial t}=-\frac{\partial}{\partial x}\left[(a_0-\Gamma)x+\Gamma\frac{x}{1+x'^2}+\frac{P}{2x}+\frac{P'_e}{2}x\right]Q_t+\frac{\partial^2}{\partial x^2}\left[\frac{P}{2}+\frac{P'_e}{2}x^2\right]Q_t. \tag{47}$$

We see from (47) that the amplitude-dependent drift coefficient $F(x)$ has the form

$$F(x)=(a_0-\Gamma)x+\Gamma\frac{x}{1+x'^2}+\frac{P}{2x}+\frac{P'_e}{2}x=a_0x-\Gamma\frac{xx'^2}{1+x'^2}+\frac{P'_e}{2}x \tag{48}$$

and the amplitude-dependent diffusion coefficient $D(x)$ is

$$D_{(x)}=\frac{P}{2}+\frac{P'_e}{2}x. \tag{49}$$

It follows from the approximate methods of paper I that the approximate formulas of the mean, variance, and skewness of FPTD are given by

$$\langle t\rangle=\langle t\rangle_q+\langle t\rangle_p=\frac{1}{2a_0}\left[C+\ln\frac{I_0}{1-I_0}+\ln\frac{a_0^2}{k(\Gamma-a_0)P}-\frac{a_0}{\Gamma-a_0}\ln(1-I_0)\right], \tag{50}$$

$$\begin{aligned}\langle(\Delta t)^2\rangle&=\langle(\Delta t)^2\rangle_q+\langle(\Delta t)^2\rangle_p\\&=\frac{1}{(2a_0)^2}\left[\frac{\pi^2}{6}+\frac{2p_e'}{a_0}\left[\frac{\frac{3}{2}-I_0-\frac{3}{2}\frac{a_0}{a_0-\Gamma}+\frac{3}{2}\left[\frac{a_0}{a_0-\Gamma}\right]^2-\frac{1}{2}\left[\frac{a_0}{a_0-\Gamma}\right]^3}{(1-I_0)^2}-3\left[\frac{a_0}{a_0-\Gamma}\right]^2\frac{1}{1-I_0}\right.\right.\\&\quad+2\left[\frac{a_0}{a_0-\Gamma}\right]^3\frac{1}{1-I_0}+\ln\frac{I_0}{1-I_0}+\left[\frac{a_0}{a_0-\Gamma}\right]^3\ln(1-I_0)-\frac{3}{2}\\&\quad\left.\left.+\frac{3}{2}\left[\frac{a_0}{a_0-\Gamma}\right]+\frac{3}{2}\left[\frac{a_0}{a_0-\Gamma}\right]^2+\frac{3}{2}\left[\frac{a_0}{a_0-\Gamma}\right]^3+\ln\frac{a_0P_e'}{k(\Gamma-a_0)P}\right]\right],\end{aligned} \tag{51}$$

and

$$\begin{aligned}\langle(\Delta t)^3\rangle&=\langle(\Delta t)^3\rangle_q+\langle(\Delta t)^3\rangle_p\\&=\frac{1}{(2a_0)^3}\left[3\left[\sum_{j=1}^{\infty}\frac{1}{j^3}-\frac{\pi^2\ln2}{3}+2\sum_{j=1}^{\infty}\frac{1}{j^2}\sum_{n=1}^{2j-1}\frac{1}{2^n n}\right]\right.\\&\quad+12\left[\frac{P_e'}{a_0}\right]^2\left\{\left[\left(\tfrac{25}{12}-\tfrac{13}{3}I_0+\tfrac{7}{2}I_0^2-I_0^3\right)\frac{1}{(1-I_0)^4}-\tfrac{25}{12}+\ln\frac{I_0}{1-I_0}+\ln\frac{a_0P_e'}{k(\Gamma-a_0)P}\right]\right.\\&\quad+\left[-\frac{5}{4}\frac{a_0}{a_0-\Gamma}\frac{1}{(1-I_0)^4}+\frac{5}{4}\frac{a_0}{a_0-\Gamma}\right]\\&\quad+\left[\frac{a_0}{a_0-\Gamma}\right]^2\left[\left[\frac{5}{2}\frac{1}{(1-I_0)^4}+\frac{5}{3}\frac{1}{(1-I_0)^3}\right]I_0^2+\frac{5}{6}\frac{1}{(1-I_0)^2}\right.\\&\qquad\left.-\frac{5}{3}\frac{1}{1-I_0}+\frac{5}{6}\right]+\frac{5}{2}\left[\frac{a_0}{a_0-\Gamma}\right]^3\frac{I_0^3(\frac{4}{3}-I_0)}{(1-I_0)^4}\\&\quad+\frac{5}{4}\left[\frac{a_0}{\Gamma-a_0}\right]^4\frac{I_0^4}{(1-I_0)^4}\\&\quad+\left[\frac{a_0}{a_0-\Gamma}\right]^5\left[I_0^5\left[\frac{1}{4(1-I_0)^4}-\frac{1}{6(1-I_0)^3}+\frac{1}{12}\frac{1}{(1-I_0)^2}\right]\right.\\&\qquad\left.\left.\left.-\frac{1}{4(1-I_0)}+\frac{I_0^4}{4}-\frac{I_0^3}{3}+\frac{I_0^2}{2}+I_0+\ln(1-I_0)\right]\right\}\right].\end{aligned} \tag{52}$$

B. Model *B*

The BFPE (33) can be rewritten as

$$\frac{\partial Q_t}{\partial t}=-\frac{\partial}{\partial x}F(x)Q_t+\frac{\partial^2}{\partial x^2}D(x)Q_t\ , \tag{53}$$

where

$$F(x)=(a_0-\Gamma)x+\Gamma\frac{x}{1+x'^2}+\frac{P_e'}{2}\frac{x}{(1+x'^2)^2}-P_e'\frac{xx'^2}{(1+x'^2)^3}\ , \tag{54}$$

$$D(x)=\frac{P}{2}+\frac{P_e'}{2}\frac{x^2}{(1+x'^2)^2}\ . \tag{55}$$

Similarly, the corresponding approximate formulas of the variance and skewness of FPTD are

$$\langle(\Delta t)^2\rangle=\langle(\Delta t)^2\rangle_q+\langle(\Delta t)^2\rangle_p$$
$$=\frac{1}{(2a_0)^2}\left[\frac{\pi^2}{6}+\frac{2P_e'}{a_0}\left[\frac{\frac{3}{2}-I_0}{(1-I_0)^2}+\ln\frac{I_0}{1-I_0}-\frac{3}{2}+\ln\frac{a_0P_e'}{k(\Gamma-a_0)P}-\frac{a_0}{2(a_0-\Gamma)}\frac{1}{(1-I_0)^2}+\frac{a_0}{2(a_0-\Gamma)}\right]\right] \tag{56}$$

and

$$\langle(\Delta t)^3\rangle=\langle(\Delta t)^3\rangle_q+\langle(\Delta t)^3\rangle_p$$
$$=\frac{1}{(2a_0)^3}\left[3\left[\sum_{j=1}^{\infty}\frac{1}{j^3}-\frac{\pi^2\ln 2}{3}+2\sum_{j=1}^{\infty}\frac{1}{j^2}\sum_{n=1}^{2j-1}\frac{1}{2^n n}\right]\right.$$
$$+12\left[\frac{P_e'}{a_0}\right]^2\left[\left(\frac{25}{12}-\frac{13}{3}I_0+\frac{7}{2}I_0^2-I_0^3\right)\frac{1}{(1-I_0)^4}+\ln\frac{I_0}{1-I_0}-\frac{25}{12}+\ln\frac{a_0P_e'}{k(\Gamma-a_0)P}\right.$$
$$\left.\left.-\frac{a_0}{4(a_0-\Gamma)}\frac{1}{(1-I_0)^4}+\frac{a_0}{4(a_0-\Gamma)}\right]\right]. \tag{57}$$

C. Colored cubic model

Similarly, the approximate analytic expressions of the mean, variance and skewness of FPTD are as follows:

$$\langle t\rangle=\frac{1}{(2a_0)}\left[C+\ln\frac{a_0^2}{PA}+\ln\frac{I_0}{1-I_0}\right], \tag{58}$$

$$\langle(\Delta t)^2\rangle=\frac{1}{(2a_0)^2}\left[\frac{\pi^2}{6}+\frac{2P_e'}{a_0}\left[\frac{\frac{3}{2}-I_0}{(1-I_0)^2}+\ln\frac{I_0}{1-I_0}-\frac{3}{2}+\ln\frac{a_0P_e'}{AP}\right]\right], \tag{59}$$

$$\langle(\Delta t)^3\rangle=\frac{1}{(2a_0)^3}\left[3\left[\sum_{j=1}^{\infty}\frac{1}{j^3}=\frac{\pi^2\ln 2}{3}+2\sum_{j=1}^{\infty}\frac{1}{j^2}\sum_{n=1}^{2j-1}\frac{1}{2^n n}\right]\right.$$
$$\left.+12\left[\frac{P_e'}{a_0}\right]^2\left[\left(\frac{25}{12}-\frac{13}{3}I_0+\frac{7}{2}I_0^2-I_0^3\right)\frac{1}{(1-I_0)^4}+\ln\frac{I_0}{1-I_0}-\frac{25}{12}+\ln\frac{a_0P_e'}{AP}\right]\right], \tag{60}$$

where $A=k\Gamma$.

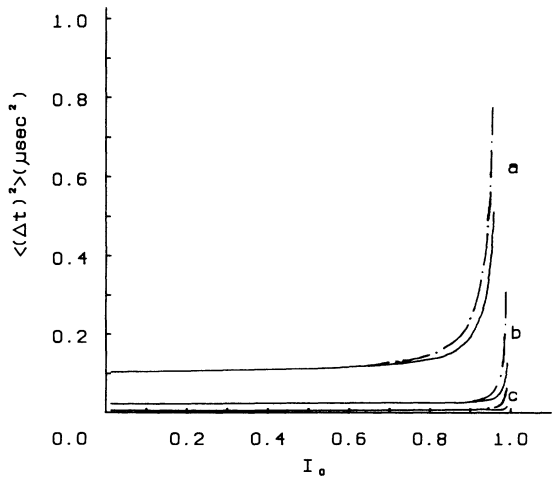

FIG. 1. The effect of saturation [Eq. (51)] on the variance of FPTD. ——, colored cubic model [Eq. (59)]; —·—·—·, model A [Eq. (51)]. Curve a, $a_0=2.16\times10^6$ sec^{-1}; curve b, $a_0=4.32\times10^6$ sec^{-1}; curve c, $a_0=8.64\times10^6$ sec^{-1}. The other laser parameters are those of set B.

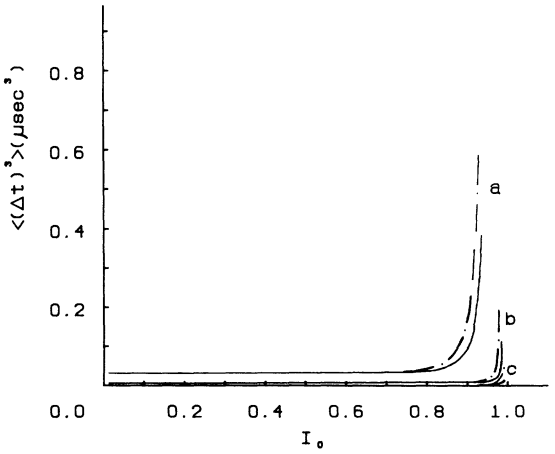

FIG. 2. The effect of saturation [Eq. (52)] on the skewness of FPTD. ——, colored cubic model [Eq. (60)]; —·—·—·, model A [Eq. (52)]. Curve a, $a_0=2.16\times10^6$ sec^{-1}; curve b, $a_0=4.32\times10^6$ sec^{-1}; curve c, $a_0=8.64\times10^6$ sec^{-1}. The other laser parameters are those of set B.

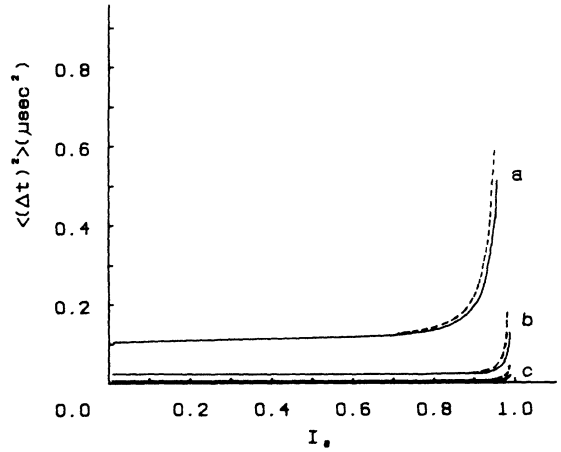

FIG. 3. The effect of saturation [Eq. (56)] on the variance of FPTD. ——, colored cubic model [Eq. (59)]; — — —, model B [Eq. (56)]. Curve a, $a_0=2.16\times10^6$ sec^{-1}; curve b, $a_0=4.32\times10^6$ sec^{-1}; curve c, $a_0=8.64\times10^6$ sec^{-1}. The other laser parameters are those of set B.

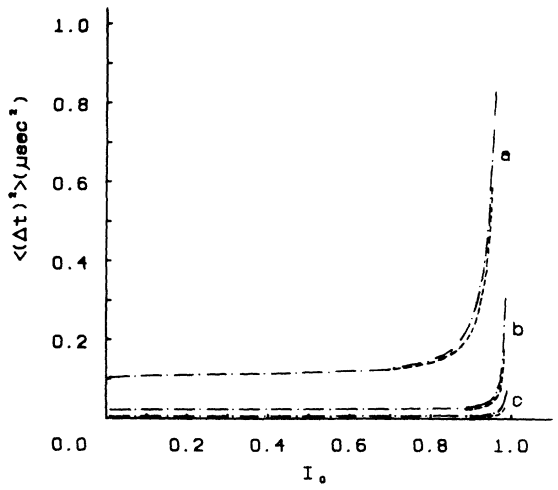

FIG. 5. The effect of saturation [Eqs. (51) and (56)] on the variance of FPTD. —·—·—·, model A [Eq. (51)]; — — —, model B [Eq. (56)]. Curve a, $a_0=2.16\times10^6$ sec^{-1}; curve b, $a_0=4.32\times10^6$ sec^{-1}; curve c, $a_0=8.64\times10^6$ sec^{-1}. The other laser parameters are those of set B.

VI. CONCLUSIONS

By means of comparing the resulting explicit formulas of the variance and skewness of FPTD for the three models we treated, important conclusions are drawn. It should be pointed out that the mean of FPTD for all the saturation models we treated has the same expression in the approximation as can be seen from the corresponding formula, so no plot needs to be made. The conclusions of this paper are as follows.

A. Comparing saturation model A with the cubic model

In Figs. 1 and 2, the curves of $\langle(\Delta t)^2\rangle$ and $\langle(\Delta t)^3\rangle$ obtained from Eqs. (54), (55), (59), and (60) with three different pump levels (a) $a_0=2.16\times10^6$ sec^{-1}, (b) $a_0=4.32\times10^6$ sec^{-1}, and (c) $a_0=8.64\times10^6$ sec^{-1} have been plotted as a function of the relative intensity I_0. The other laser parameters are those of set B given in Refs. [3] and [8]. That is, $A=2.64\times10^6$ sec^{-1}, $P=0.0043$ sec^{-1}, $P'=3\times10^4$ sec^{-1}, and $\gamma=2.4\times10^6$ sec^{-1}. These curves show that in the regime $0<I_0<0.8$, saturation model A and the cubic model cannot be distinguished. However, in the regime $0.8<I_0<1$, as the laser intensity is increased, the increase of variance and skewness of saturation model A is faster than that of the cubic model. Comparing Figs. 1 and 2 with Figs. 7(b) and 7(c) of Ref. [3], respectively, we conclude that our analytic results show good agreement with numerical simulation.

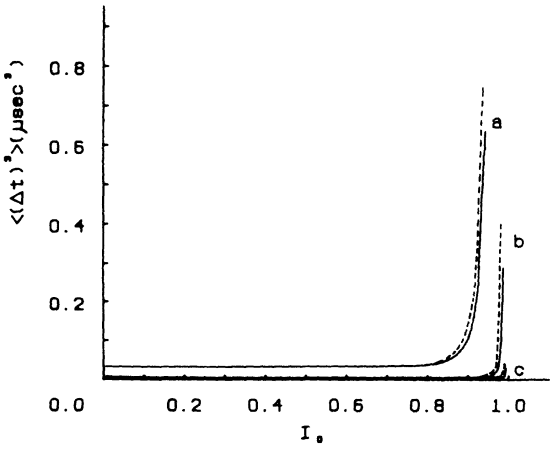

FIG. 4. The effect of saturation [Eq. (57)] on the skewness of FPTD. ——, colored cubic model [Eq. (60)]; — — —, model B [Eq. (57)]. Curve a, $a_0=2.16\times10^6$ sec^{-1}; curve b, $a_0=4.32\times10^6$ sec^{-1}; curve c, $a_0=8.64\times10^6$ sec^{-1}. The other laser parameters are those of set B.

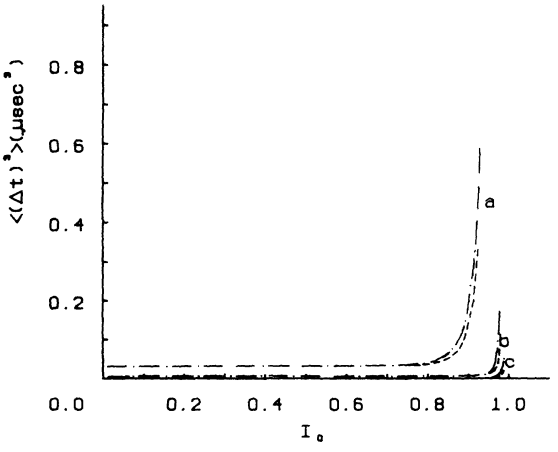

FIG. 6. The effect of saturation [Eqs. (52) and (57)] on the skewness of FPTD. —·—·—·, model A [Eq. (52)]; — — —, model B [Eq. (57)]. Curve a, $a_0=2.16\times10^6$ sec^{-1}; curve b, $a_0=4.32\times10^6$ sec^{-1}; curve c, $a_0=8.64\times10^6$ sec^{-1}. The other laser parameters are those of set B.

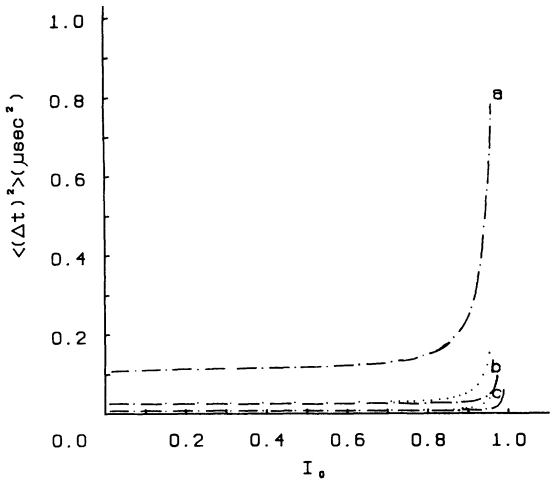

FIG. 7. The effect of saturation [Eq. (51) and Eq. (40) in paper I] on the variance of FPTD. —·—·—·, colored model A [Eq. (51)]; · · · ·, white model A [Eq. (40) in paper I]. Curve a, $a_0=2.16\times10^6$ sec^{-1}; curve b, $a_0=4.32\times10^6$ sec^{-1}; curve c, $a_0=8.64\times10^6$ sec^{-1}. The other laser parameters are those of set B. In curves a the curves of both colored model A and white model A are concurrent.

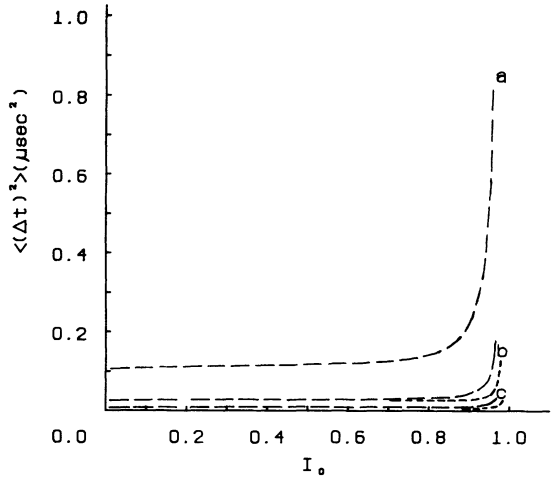

FIG. 9. The effect of saturation [Eq. (56) and Eq. (46) in paper I] on the variance of FPTD. — — —, colored model B [Eq. (56)]; — — —, white model B [Eq. (46) in paper I]. Curve a, $a_0=2.16\times10^6$ sec^{-1}; curve b, $a_0=4.32\times10^6$ sec^{-1}; curve c, $a_0=8.64\times10^6$ sec^{-1}. The other laser parameters are those of set B. In curves a, the curves of both colored and white models B are concurrent.

B. Comparing saturation model B with the cubic model

The curves of $\langle(\Delta t)^2\rangle$ and $\langle(\Delta t)^3\rangle$ obtained from Eqs. (56), (57), (59), and (60) have been plotted in Figs. 3 and 4. These curves show $\langle(\Delta t)^2\rangle$ and $\langle(\Delta t)^3\rangle$ for the three pump levels. From Figs. 3 and 4 we clearly see that in the regime $0<I_0<0.8$, model B and the cubic model cannot be distinguished. However, in the regime $0.8<I_0<1$ as the laser intensity is increased, although the increase of the variance and skewness for saturation model B is faster than that of the cubic model, but the increase of variance and skewness in the colored-gain-noise model (model B) are slower than those obtained from the colored-loss-noise model (model A). Therefore, the prefactor of the pump fluctuation term in model B seems to play a curb role in the increase of the variance and skewness. For the advantage of comparison, we have plotted the curves of $\langle(\Delta t)^2\rangle$ for both models A and B in Fig. 5. Similarly, the curves of $\langle(\Delta t)^3\rangle$ are plotted in Fig. 6.

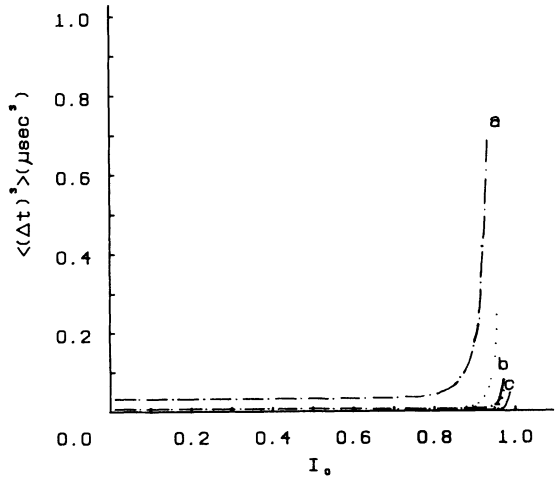

FIG. 8. The effect of saturation [Eq. (52) and Eq. (43) in paper I] on the skewness of FPTD. —·—·—·, colored model A [Eq. (52)]; · · · ·, white model A [Eq. (43) in paper I]. Curve a, $a_0=2.16\times10^6$ sec^{-1}; curve b, $a_0=4.32\times10^6$ sec^{-1}; curve c, $a_0=8.64\times10^6$ sec^{-1}. The other laser parameters are those of set B. In curves a, the curves of both colored model A and white model A are concurrent.

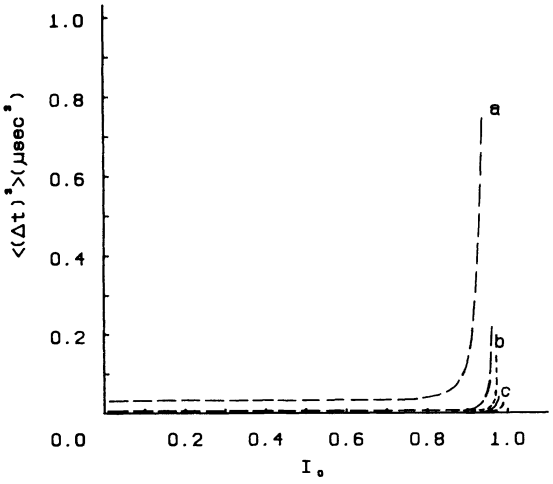

FIG. 10. The effect of saturation [Eq. (57) and Eq. (47) in paper I] on the skewness of FPTD. — — —, colored model B [Eq. (57)]; — — —, white model B [Eq. (47) in paper I]. Curve a, $a_0=2.16\times10^6$ sec^{-1}; curve b, $a_0=4.32\times10^6$ sec^{-1}; curve c, $a_0=8.64\times10^6$ sec^{-1}. The other laser parameters are those of set B. In curves a, the curves of both colored and white models B are concurrent.

C. Effects of the noisy color in the laser transient of the saturation models

From Figs. 7–10, we clearly see that in the regime $0 < I_0 < 0.8$, the colored saturation model and the white saturation model still cannot be distinguished. But in the regime $0.8 < I_0 < 1$, as the laser intensity is increased, the increase of the variance and skewness for saturation model A (B) with colored noise are slower than those of saturation model A (B) with white noise. Moreover, due to the influence of the prefactor of the pump fluctuation term, the difference between the colored-gain-noise model and the white-gain-noise model has become small. The same influence also occurs in the skewness.

Finally, it must be pointed out that the stochastic behavior of dye lasers has become the main focus of interest for many investigators. To get an effective Fokker-Planck equation from the dynamical equation driven by colored noise, a number of theories have been proposed. However, the conventional theories are restricted to the small correlation time of the colored noise [5,9]. Recently, Jung and Hanggi have developed a unified colored-noise theory which does not restrict the value of the correlation time of the noise [10,11]. In a separate paper, we have studied the same problems treated in this paper by virtue of the unified colored theory [10] and make a comparison between the theories mentioned above. In this paper we have confined ourself to use the BFPE formulas to calculate the mean, variance, and skewness of the FPTD for the colored-noise models only.

---

*Also at Institute of Theoretical Physics, Academia Sinica, P.O. Box 2735, Beijing, People's Republic of China.
†Mailing address.

[1] Li Cao, Da-jinn, Wu, and Xue-li Luo, preceding paper, Phys. Rev. A **44**, 6838 (1992).
[2] E. Peacock-Lopez, F. J. de la Rubia, B. J. West, and K. Lindenberg, Phys. Rev. A **39**, 4026 (1989).
[3] S. Zhu, A. W. Yu, and R. Roy, Phys. Rev. A **34**, 4333 (1986).
[4] J. M. Sancho, M. S. Miguel, H. Yamazaki, and T. Kawakubo, Physica **116A**, 560 (1982).
[5] J. M. Sancho, M. S. Miguel, S. L. Katz, and J. D. Gunton, Phys. Rev. A **26**, 1589 (1982).
[6] K. Lindenberg and B. J. West, Physica **119A**, 485 (1983); **128A**, 25 (1984).
[7] K. Lindenberg, B. J. West, and J. Masoliver, in *Noise in Nonlinear Dynamical Systems,* edited by F. Moss and P. V. E. McClintock (Cambridge University Press, Cambridge, 1989).
[8] S. Zhu, Phys. Rev. A **41**, 1689 (1990).
[9] R. F. Fox, Phys. Rev. A **33**, 467 (1986); 34, 4525 (1986).
[10] P. Jung and P. Hanggi, Phys. Rev. A **35**, 4464 (1987); J. Opt. Soc. Am. B **5**, 979 (1988); Phys. Rev. Lett. **61**, 11 (1988).
[11] P. Hanggi, P. Jung, and F. Marchesoni, J. Stat. Phys. **54**, 1367 (1989).